A LOCAL AVERAGE METHOD FOR STOCHASTIC THERMAL ANALYSIS UNDER HEAT CONDUCTION CONDITIONS

by

Tao WANG[a,b*], Guoqing ZHOU[a], Jianzhou WANG[a], and Leijian YIN[b]

[a] State Key Laboratory for Geomechanics and Deep Underground Engineering, China University of Mining and Technology, Xuzhou, Jiangsu, China
[b] School of Mechanics and Civil Engineering, China University of Mining and Technology, Xuzhou, Jiangsu, China

Original scientific paper
https://doi.org/10.2298/TSCI170113181W

In this paper, a new triangular discretization method for 2-D random field is proposed, and the computational formula of the covariance for any two triangular random field elements is developed. Its main advantage, compared to the quadrilateral discretization method, is that triangular local average method can perfectly combine with the triangular finite element method. Also, the corresponding relation is clearer and the computer codes are simpler. Based on the new local average method, a numerical analysis for random temperature field of geotechnical structures under heat conduction conditions is presented by the Monte-Carlo method, and the computational formulas of mathematical expectation matrix and standard deviation matrix are provided. A series of computer codes have been compiled by Matrix Laboratory software. A numerical example is presented to demonstrate the random effects of uncertain parameters, and the accurateness of the proposed approach is proven by comparing these results with the results derived from quadrilateral local average method.

Key words: *uncertain thermal properties, random fields, local average method, triangular elements, geotechnical structures*

Introduction

Thermal effects are important factors to be considered in many scientific and engineering problems [1, 2]. Generally, a temperature change can cause a change of pore-fluid density, so that buoyancy-driven flow, which is also called the convective pore-fluid flow, can take place in the fluid-saturated porous medium [3-5]. Since the buoyancy-driven flow can affect the thermal field distribution through heat convection, it is strongly coupled with the thermal field in both geological and engineering length-scales [6-8]. More importantly, such convective pore-fluid flow in saturated porous media can result in the formation of large mineral deposits within the crustal rocks [1] and large geological faults [9, 10]. In addition, thermal effects can also play an important role in geochemical reactions [11, 12]. On the other hand, the deformation of a porous medium can cause a considerable change in the porosity and permeability of the porous medium [2]. Since both the physical dissolution [13, 14] and the chemical dissolution [15, 16] of dissolvable materials in fluid-saturated porous media can cause a significant change in the porosity and permeability of the porous media, they can affect the pore-fluid flow through the change of flow channels [17, 18]. This indicates that

* Corresponding author, e-mail: wtbtj@126.com

chemical dissolution reactions are strongly coupled with the pore-fluid flow through porosity and permeability change [19-22], and indirectly coupled with the thermal field because the thermal field is strongly coupled with the pore-fluid flow. Therefore, fully coupled problems between medium deformation, pore-fluid flow, heat transfer, mass transport, and chemical reactions can be found in a wide range of scientific and engineering problems [23]. For this reason, any improvement on the existing methods of predicting the thermal field distribution in fluid-saturated porous media may have both scientific and practical significance [1-23]. In a broad sense, the outcome of such an improvement can enrich the contents of the emerging computational geoscience [2].

For some geotechnical structures, it is very important to numerically analyze the thermal stability for engineering construction. Traditionally thermal stability analyses have been conducted by solving the heat conduction equation under the assumption that the soil properties are deterministic [24-27]. In fact, especially for geotechnical structures, there are a large number of uncertainties for soil properties [28-31]. Therefore, it is reasonable to take into account the probabilistic aspects of the soil parameters. In the early time, some researchers tried to simulate random parameters as random variables [32-35]. Conventional deterministic temperature field analysis becomes uncertain temperature field analysis including random variables. Xiu and Karniadakis [36], and Emery [37] gave the description of the random parameters based on the stochastic progress theory. However, both the random variable method and the stochastic progress method cannot describe the spatial variability of soil parameters. Vanmarcke and Grigoriu [38] and Vanmarcke [39] first pointed out that the random field method can accurately describe the spatial variability of soil parameters.

To consider the random field, discretization is necessary. The local average method is popular because it converges rapidly and it needs less statistical information than other methods. Vanmarcke *et al.* [40] presented a rectangular local average method to discretize 2-D random field. Chen and Dai [41] presented an arbitrary quadrilateral local average method based on the theory of linear co-ordinate transformation. Although the quadrilateral local average method can combine with the quadrilateral finite element method, *e. g.*, figs. 1(a) and 1(c), it is difficult to combine with the more popular triangular finite element method. It is because that the quadrilateral random field grids cannot match up with the triangular finite element grids, *e. g.*, figs. 1(b) and 1(c). Therefore, the triangular local average method is necessary, *e. g.*, fig. 1(d), and the triangular random field grids can combine with the triangular finite element grids, *e. g.*, figs. 1(b) and 1(d).

Because the calculation of random temperature fields including random fields is unusual, there is less research on this aspect. Liu *et al.* [42, 43] calculated the random temperature field of a frozen soil roadbed based on the random field theory. But a detailed description of the random field and the numerical characteristics of local average random field were not given. Wang and Zhou [44] compared the results of calculating temperature field by modeling uncertain material parameters as spatially random fields and traditional random variables respectively. But there is still no complete understanding of the random effects of uncertain thermal parameters.

In this paper, the uncertain thermal parameters (thermal conductivity and volumetric heat capacity) are modeled as spatially continuous random fields. A new triangular local average method is presented based on local average theory. Its main advantage, compared to the quadrilateral local average method, is that triangular random field grids can perfectly match up with triangular finite element grids. Finally, the random temperature fields of a geotechnical structure are studied *via* Monte-Carlo stochastic finite element method. The result can

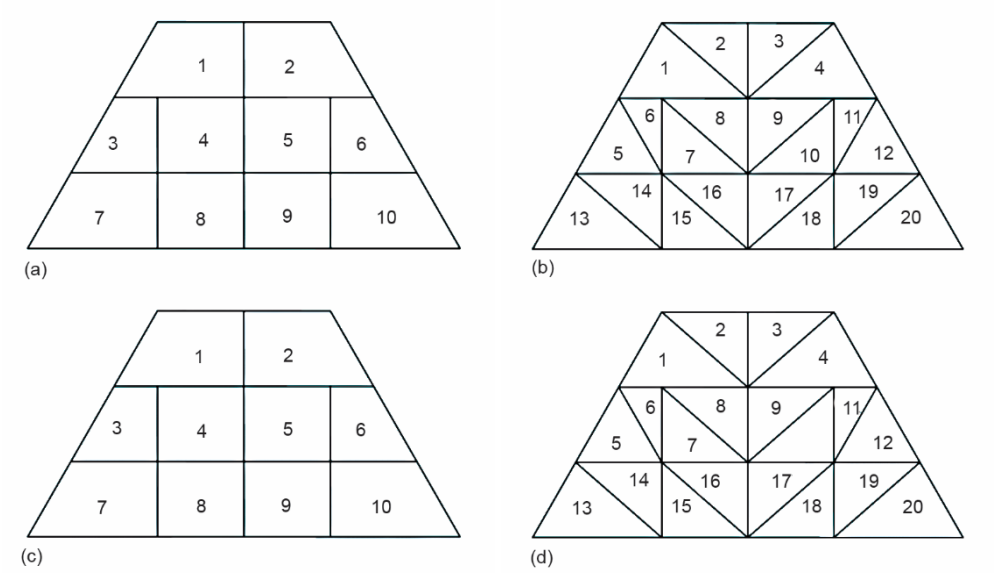

Figure 1. Matching relation between finite element mesh and random field mesh; (a) quadrangular finite element grids, (b) triangular finite element grids, (c) quadrilateral local average method [40, 41], (d) triangular local average method

improve our understanding of uncertain thermal properties of geotechnical structures under the condition of probabilistic aspects, and provide a theoretical basis for stochastic stress fields and displacement fields, indicating that the outcome of this study may enrich the research contents of the emerging computational geoscience [2].

Deterministic heat conduction problems

For the 2-D heat conduction problem of the temperature field (without considering the rate of internal heat generation), the basic equation can be written:

$$\frac{\partial}{\partial x}\left(k\frac{\partial T}{\partial x}\right)+\frac{\partial}{\partial y}\left(k\frac{\partial T}{\partial y}\right)=C\frac{\partial T}{\partial t} \tag{1}$$

where T is the temperature, t – the time, k – the thermal conductivity, C – the volumetric heat capacity, and x, y – the position co-ordinate.

Based on the backward difference method, the finite element equations of the heat transfer can be written:

$$\left([\boldsymbol{K}]+\frac{[\boldsymbol{N}]}{\Delta t}\right)\{\boldsymbol{T}\}_t=\frac{[\boldsymbol{N}]}{\Delta t}\{\boldsymbol{T}\}_{t\text{-}\Delta t}+\{\boldsymbol{P}\}_t \tag{2}$$

where $[\boldsymbol{K}]$ is the stiffness matrix, $[\boldsymbol{N}]$ – the unsteady temperature matrix, Δt – the time step, $\{\boldsymbol{T}\}_t$ – the column vector of temperature, $\{\boldsymbol{P}\}_t$ – the right column vector, and t – the same time of every column vector.

According to Lewis *et al.* [45], the detailed calculation formulas of $[\boldsymbol{K}]$, $[\boldsymbol{N}]$, and $\{\boldsymbol{P}\}_t$ can be obtained. Both $[\boldsymbol{K}]$, $[\boldsymbol{N}]$, and $\{\boldsymbol{P}\}_t$ are deterministic variables in the conventional

deterministic finite element analysis, so $\{\boldsymbol{T}\}_t$ of eq. (2) is a deterministic result. In this paper, $[\boldsymbol{K}]$ and $[\boldsymbol{N}]$ are not deterministic variables because the thermal parameters are uncertain, so $\{\boldsymbol{T}\}_t$ of eq. (2) also is a random result. It is more accurate by modeling the uncertain thermal properties as spatially random fields instead of conventional random variables [46].

Calculation models of stochastic parameters

Description of random field

The essence of the random field model is that uncertain stochastic parameters are modeled as homogeneous Gaussian random fields and the correlation of the uncertain parameters are described by autocorrelation function. It is a method to calculate the spatial average variance from just the point variance based on the test data. We modeled the thermal conductivity and volumetric heat capacity as a 2-D continuous random field. The $P(x, y)$ is a point on the plane, and the random function, $X(P)$, constitutes a 2-D continuous random field. Assuming $E[X(x, y)] = m$, and $\mathrm{Var}[X(x, y)] = \sigma^2$.

Based on the random field theory, the autocorrelation function can be written:

$$R_X[P,P'] = E[X(P)X(P')] = R_X(|x-x'|,|y-y'|) \tag{3}$$

where the position of $P'(x', y')$ is different from $P(x, y)$.

The standard relevant coefficient can be written:

$$\rho[P,P'] = \frac{R_X[P,P']}{\sigma^2} = \rho(|x-x'|,|y-y'|) \tag{4}$$

where $\rho(\xi, \eta)$ is a standard relevant coefficient.

The $X(P)$ is a random field whose mathematical expectation is μ. We assume that $Y(P) = X(P) - \mu$, so $Y(P)$ is a random field whose mathematical expectation is zero. The mathematical expectation, variance and covariance of $Y(P)$ are:

$$E[Y(P)] = E[X(P) - \mu] = E[X(P)] - \mu = 0 \tag{5}$$

$$\mathrm{Var}[Y(P)] = D[X(P) - \mu] = D[X(P)] = \sigma^2 \tag{6}$$

$$\mathrm{Cor}[Y_i(P), Y_j(P)] = E\{[Y_i(P) - E(Y_i(P))][Y_j(P) - E(Y_j(P))]\} =$$

$$= E[Y_i(P)Y_j(P)] = E\{[X_i(P) - \mu][X_j(P) - \mu]\} = Cor[X_i(P), X_j(P)] \tag{7}$$

Therefore, it is reasonable when we assume that the mean function is zero for the analysis of the numerical characteristics of the local average random field.

A new triangular local average method

Although the triangular finite element method is popular, the conventional quadrilateral local average method cannot combine with it. It is because that the quadrilateral random field grids cannot match up with the triangular finite element grids. Therefore, we present a new triangular local average method to discretize 2-D random field.

The $X(x,y)$ is a 2-D continuous random field for uncertain stochastic parameters. The mathematical expectation is zero and the variance is constant, *i. e.*, $E[X(x\ y)] = 0$ and

Var[$X(x\ y)$] = σ^2. It is the triangular local average method when the 2-D random field is divided by triangular grids. The triangular random field element is shown in fig. 2.

The local average random field for a triangular element is defined:

$$X_e = \frac{1}{A_e}\int_{\Omega_e} X(x,y)\mathrm{d}x\mathrm{d}y \tag{8}$$

where A_e is the area of e and Ω_e – the possessive section of e.

The mathematical expectation of the local average random field for a triangular element is:

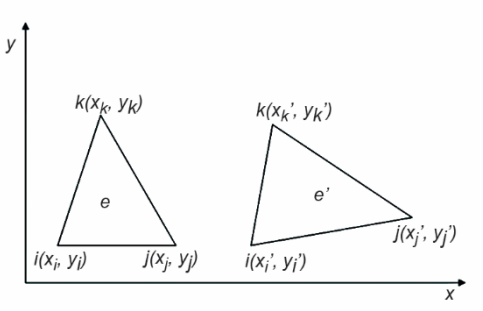

Figure 2. The 2-D triangular random field elements

$$E(X_e) = E\left[\frac{1}{A_e}\int_{\Omega_e} X(x,y)\mathrm{d}x\mathrm{d}y\right] = 0 \tag{9}$$

The covariance of the local average random field for two triangular elements is:

$$\mathrm{Cov}(X_e, X_{e'}) = E\left[(X_e - m)(X_{e'} - m)\right] = E(X_e X_{e'}) \tag{10}$$

According to eqs. (3), (4), and (8), eq. (10) can be renewed:

$$\mathrm{Cov}(X_e, X_{e'}) = \frac{\sigma^2}{A_e A_{e'}}\int_{\Omega_e}\int_{\Omega_{e'}} \rho(|x-x'|,|y-y'|)\mathrm{d}x\mathrm{d}x'\mathrm{d}y\mathrm{d}y' \tag{11}$$

where $A_{e'}$ is the area of e', and Ω_e' is the possessive section of e'.

According to eq. (9), we can see the mathematical expectation of the local average random field for an triangular element is same as the original random field and its calculated value is zero. The covariance of the local average random field for two triangular elements is complicated for calculating. It is difficult to obtain the explicit formulation of eq. (11) when the calculation formula of standard relevant coefficient is complicated, so the co-ordinates transform method and the Gauss numerical method are needed to perform the integration.

Based on co-ordinates transform method, x, y, x' and y' can be expressed:

$$\begin{cases} x = N_i(x_i - x_k) + N_j(x_j - x_k) + x_k \\ y = N_i(y_i - y_k) + N_j(y_j - y_k) + y_k \\ x' = N_i'(x_i' - x_k') + N_j'(x_j' - x_k') + x_k' \\ y' = N_i'(y_i' - y_k') + N_j'(y_j' - y_k') + y_k' \end{cases} \tag{12}$$

where N_i and N_j are the shape function of e, N_i', and N_j' is the shape function of e'.

According to eq. (12), eq. (11) can be rewritten:

$$\mathrm{Cov}(X_e, X_{e'}) = \frac{\sigma^2}{A_e A_{e'}}\int_{\Omega_{e'}}\int_{\Omega_e} g(N_i, N_j, N_k, N_i', N_j', N_k')\mathrm{d}\Delta\mathrm{d}\Delta' \tag{13}$$

where $g(N_i, N_j, N_k, N_i', N_j', N_k') = \rho(|x - x'|, |y - y'|)$.

Based on Gauss numerical method, there is:

$$\iint_{\Delta} g(N_i, N_j, N_k)\,\mathrm{d}\Delta = \Delta \sum_{K=1}^{M} \omega^{(K)} g[N_i^{(K)}, N_j^{(K)}, N_k^{(K)}] \tag{14}$$

where Δ is the area of triangular element, M – the number of basis points, and $\omega^{(K)}$ – the weighted coefficient.

According to eq. (14), eq. (13) can be renewed:

$$\mathrm{Cov}(X_e, X_{e'}) = \sigma^2 \sum_{K=1}^{M} \sum_{R=1}^{M} \omega^{(K)} \omega'^{(R)} g[N_i^{(K)}, N_j^{(K)}, N_k^{(K)}, N_i'^{(R)}, N_j'^{(R)}, N_k'^{(R)}] \tag{15}$$

Equation (15) is the computational formula of the covariance for two triangular random field elements. If the standard relevant coefficient is known, we can obtain the result of covariance matrix. In order to guarantee the calculation accuracy, we assume that $M = 7$, and tab. 1 is the calculating parameter for eq. (15).

Table 1. Calculating parameter for Gauss numerical method

M	1	2	3	4	5	6	7
$\omega^{(K)}[\omega'^{(R)}]$	1/20	1/20	1/20	2/15	2/15	2/15	9/20
$N_i^{(K)}[N_i'^{(R)}]$	1	0	0	0	1/2	1/2	1/3
$N_j^{(K)}[N_j'^{(R)}]$	0	1	0	1/2	0	1/2	1/3
$N_k^{(K)}[N_k'^{(R)}]$	0	0	1	1/2	1/2	0	1/3

Analysis method of random temperature field

In this paper, the sample values of each random field element can be obtained by independent transformation method [44]. The random temperature field of geotechnical structures can be calculated by eq. (2), boundary conditions, initial conditions and the samples of the local average random field based on the Monte-Carlo method. The Monte-Carlo method is accurate no matter how large the perturbations are. It can be perfectly combined with the deterministic finite element method and thus avoids the complicated theoretical derivation. It is simpler for program composition because the triangular local average method can perfectly combine with the triangular finite element method, and the random field mesh and the finite element mesh is able to use the same mesh, the corresponding relation is very clear. Therefore, the triangular local average method can be widely used to discretize 2-D random field. Although the computational load is heavy for the Monte-Carlo method, it is the most accurate method for stochastic finite element analysis and the performance of the computer is getting better and better. Also, Neumann expansion method can improve the efficiency to some extent [47]. For this paper, it is unnecessary because the numbers of finite element grid and random field grid are small.

The mathematical expectation matrix, E(T), and the standard deviation matrix, σ(T), can be obtained by statistical analysis of the temperatures of the finite element nodes. The computational formulas are:

$$\mathrm{E(T)} = \frac{1}{N}\sum_{k=1}^{N}\mathrm{T}_k \tag{16}$$

$$\sigma(T) = \sqrt{\frac{1}{N-1}\sum_{k=1}^{N}\left[\mathrm{T}_k - \mathrm{E(T)}\right]^2} = \sqrt{\frac{1}{N-1}\sum_{k=1}^{N}\left[\mathrm{T}_k\right]^2 - \frac{N}{N-1}\left[\mathrm{E}(T)\right]^2} \tag{17}$$

where $\boldsymbol{T}_k$ is the temperature matrix and N – the number of calculations.

Based on the previous analysis, a series of computer codes have been compiled by MATLAB

Numerical examples and analysis

Figure 3(a) is the section shape of a geotechnical structure. The O_1, O_2, and O_3 are three different locations on the section. For the mean value of thermal parameters, k = 2.7 W/mK, C = 2300 kJ/kgK. For the boundary of AB and CD, T_{AB} = 15 ºC, T_{CD} = 30 ºC, DA and BC are adiabatic. The initial temperature field is 5 ºC. Figure 3(b) shows the triangular finite element grids for finite element method. Figure 4 shows the quadrilateral random field grids and the triangular random field grids for local average method. It can be seen that the quadrilateral random field grids cannot match up with the triangular finite element grids from figs. 3(b) and 4(b). Figures 3(b) and 4(a) show that the triangular random field grids can perfectly match up with the triangular finite element grids because the discrete grid is the same. It is obvious that the corresponding relation is clearer and the program is simpler than conventional quadrilateral local average method. It must be pointed out that the previous boundary conditions are only suitable for the problems of finite computational domains, such as the artificially-designed problem in this study. However, since most of geoscience and geotechnical problems may involve infinite computational domains [48-50], the dynamic and transient infinite elements [51, 52] should be used to simulate the far field of such geoscience and geotechnical problems in the real world [48-50, 53-54].

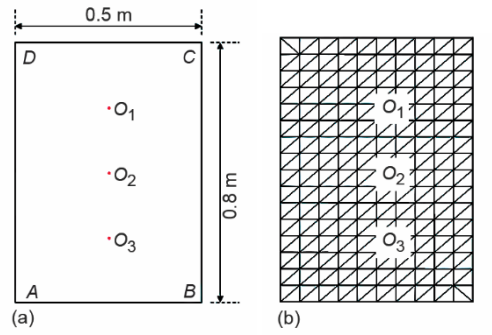

Figure 3. The computational model; (a) cross-section, (b) triangular finite element mesh

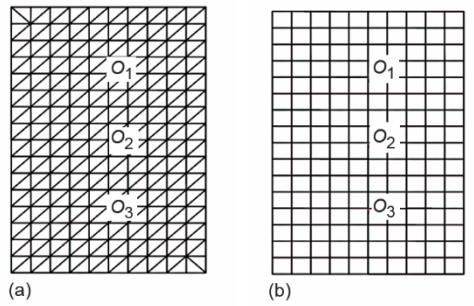

Figure 4. Random field mesh; (a) triangle, (b) quadrilateral

In order to prove the correctness of proposed approach, we compared the calculation results of two local average methods. According to Liu and Liu [55], figs. 3(b) and 4(b) have the corresponding relations which every quadrilateral random field grid contains two triangular finite element grids. The computational formulas of mathematical expectation and covariance for quadrilateral random field element can be obtained from Chen and Dai [41]. Figure

4(b) has 160 quadrilateral elements and 187 nodes while fig. 4(a) has 320 triangular elements and 187 nodes. We modeled the thermal conductivity and the volumetric heat capacity as two different random fields. Therefore, there are 320 random variables in fig. 4(b) and 640 random variables in fig. 4(a). We assumed that $\rho(r, s) = \exp[-(r + s)/50]$ and the coefficients of variation of thermal conductivity and volumetric heat capacity are both 0.2. The random temperature field can be obtained by the stochastic finite element program which is compiled by MATLAB.

Figures 5 and 6 show the results of mean temperature and standard deviation for two local average methods in 100 hours. It can be seen from figs. 5(a)-5(c) that the mean temperature is the same. The results of mean temperature are believable because the mathematical expectations of the random field element are equal for two local average methods. It can be seen from figs. 6(a)-6(c) that the standard deviation of quadrilateral local average method is smaller than the standard deviation of triangular local average method. Based on the proposed approach and Chen and Dai [41], the variances of triangular random field element are bigger. Therefore, the results of standard deviation are credible because the sample values of the quadrilateral random field element are smaller.

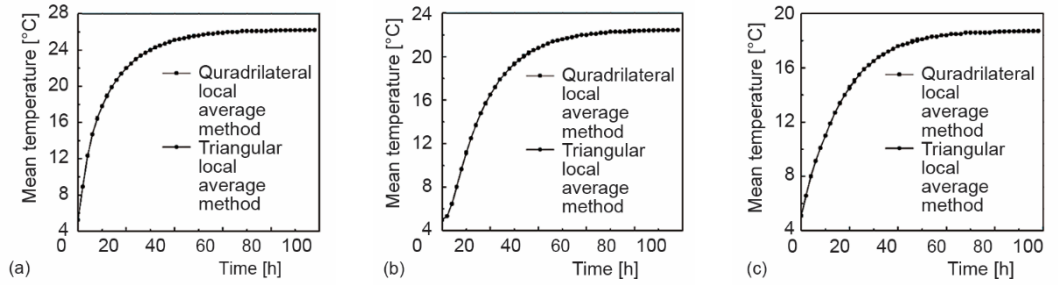

Figure 5. Mean temperature of two local average methods; (a) O_1, (b) O_2, (c) O_3

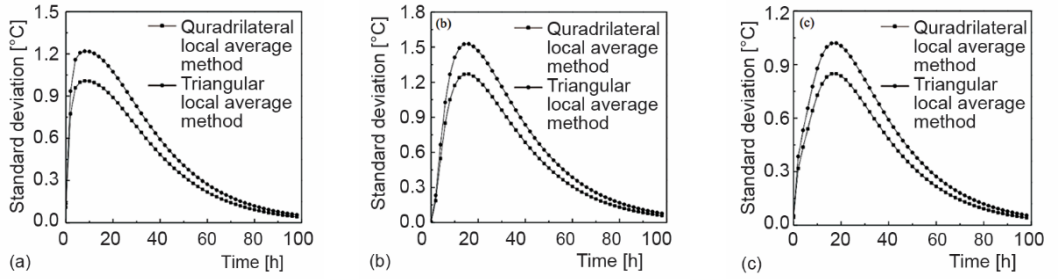

Figure 6. Standard deviation of two local average methods; (a) O_1, (b) O_2, (c) O_3

In order to study the random response of thermal conductivity and the volumetric heat capacity, we calculated different case which is listed as tab. 2.

Table 2. Different coefficient of variation

Case	1	2	3	4	5	6	7	8	9	10
Thermal conductivity	0	0.1	0.2	0.3	0	0	0	0.1	0.2	0.3
Volumetric heat capacity	0	0	0	0	0.1	0.2	0.3	0.1	0.2	0.3

Figure 7 shows the mean temperature of O_1, O_2, and O_3 in 100 hours. It can be seen from figs. 7(a)-7(c) that the same location has the same mean temperature for different cases, and the stable mean temperature of O_1 is higher than O_2, the stable mean temperature of O_2 is higher than O_3. Case 1 is the deterministic result of the temperature field because the coefficient of variation is zero. According to Bernoulli's law of large numbers, the results of mean temperature for different cases are credible.

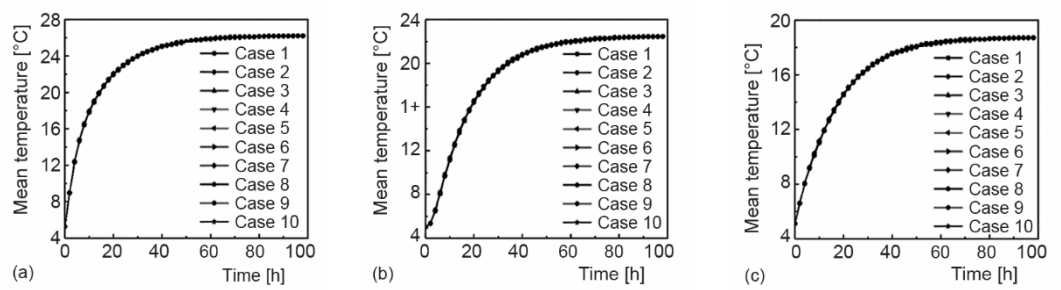

Figure 7. Mean temperature of different locations; (a) O_1, (b) O_2, (c) O_3

Figure 8 shows the standard deviation of O_1, O_2, and O_3 for the different variability of thermal conductivity in 100 hours. From figs. 8(a)-8(c), it can be seen that the larger the coefficient of variation is, the larger the standard deviation is, and different locations have different random response. For location O_1, O_2, and O_3, the standard deviation is increases first, and then decreases. For location O_1, O_2, and O_3, the maximum of standard deviation appears at the 10^{th}, 14^{th}, and 18^{th} hour, respectively. Therefore, we can conclude that the maximum of standard deviation doesn't appear at the same time for different locations. For the different variability of volumetric heat capacity, a similar conclusion can be made.

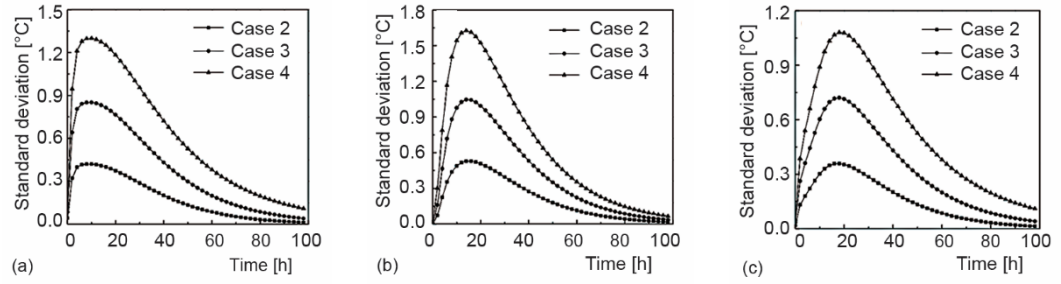

Figure 8. Standard deviation of different locations; (a) O_1, (b) O_2, (c) O_3

Figure 9 shows the standard deviation of O_2 for the same variability of thermal conductivity and volumetric heat capacity in 100 hours. From figs. 9(a)-9(c), it can be seen that the combined action of thermal conductivity and volumetric heat capacity have more strongly random response to the temperature field than any one of them. For the effects of thermal conductivity and volumetric heat capacity alone, according to fig. 9(a), the variability is roughly the same when the coefficient of variation of thermal conductivity and volumetric heat capacity is 0.1. According to fig. 9(b), there is a little different for the variability when the coefficient of variation of thermal conductivity and volumetric heat capacity is 0.2. The

influence from thermal conductivity is more strongly than volumetric heat capacity after the peak of standard deviation. According to fig. 9(c), there is significantly different for the variability when the coefficient of variation of thermal conductivity and volumetric heat capacity is 0.3. The influence from volumetric heat capacity is more strongly than thermal conductivity before the peak of standard deviation, while the influence from thermal conductivity is more strongly than volumetric heat capacity after the peak of standard deviation. Therefore, we can conclude that thermal conductivity and volumetric heat capacity have different random response to the temperature field when the coefficient of variation is larger. For the location O_1 and O_3, a similar conclusion can be made.

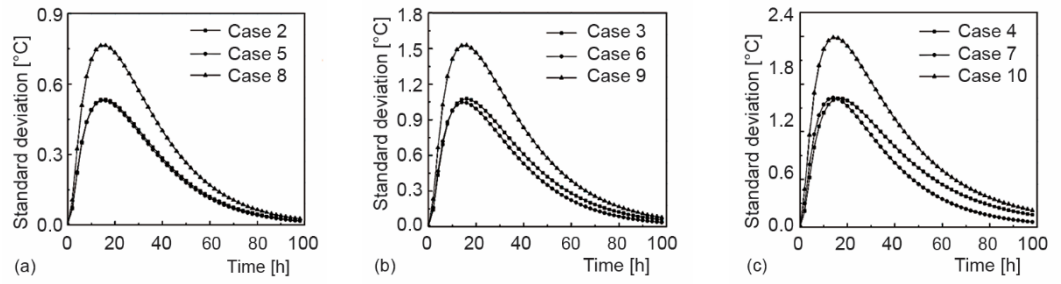

Figure 9. Standard deviation of O_2; (a) 0.1, (b) 0.2, (c) 0.3

Conclusions

According to the results from this study, the following conclusions can be drawn as follows.

- The new local average method can perfectly combine with triangular finite element method. Comparing with the traditional quadrilateral local average method, the mean temperature is the same while the standard deviation is bigger. The proposed approach has clearer corresponding relation, simpler computer codes and more accurate results.
- A stochastic finite element program compiled by MATLAB can directly output the statistical results for uncertain thermal properties. The related computer codes can be employed for other probabilistic problems after making slight modifications.
- When the coefficient of variation is large, the effect of volumetric heat capacity is more strongly than thermal conductivity before the peak of standard deviation, while the effect of thermal conductivity is more strongly than volumetric heat capacity after the peak of standard deviation.

It should be pointed out that for most scientific and engineering problems in the real world, thermal process is often coupled with the pore-fluid flow process, medium deformation process, mass transport process and chemical reactions. Since the thermal process is only considered in this study, the fully-coupled problem between medium deformation, pore-fluid flow, heat transfer, mass transport and chemical reactions [1-23] should be considered in the future research, so that the numerical method proposed in this study can be used to solve realistic scientific and engineering problems.

Acknowledgment

This research was supported by the National Natural Science Foundation of China (Grant No. 51604265) and the Fundamental Research Funds for the Central Universities (Grant No. 2017QNA30).

References

[1] Zhao, C. B., *et al.*, *Convective and Advective Heat Transfer in Geological Systems*, Springer-Verlag, Berlin, 2008
[2] Zhao, C. B., *et al.*, *Fundamentals of Computational Geoscience: Numerical Methods and Algorithms*, Springer-Verlag, Berlin, 2009
[3] Zhao, C. B., *et al.*, Theoretical Investigation of Convective Instability in Inclined and Fluid-Saturated Three-Dimensional Fault Zones, *Tectonophysics*, *387* (2004), 1-4, pp. 47-64
[4] Zhao, C. B., *et al.*, Investigating Dynamic Mechanisms of Geological Phenomena Using Methodology of Computational Geosciences: An Example of Equal-Distant Mineralization in A Fault, *Science China Earth Sciences*, *51* (2008), 7, pp. 947-954
[5] Zhao, C. B., *et al.*, Computational Simulation of Seepage Instability Problems in Fluid-Saturated Porous Rocks: Potential Dynamic Mechanisms for Controlling Mineralization Patterns, *Ore Geology Reviews*, *79* (2016), Dec., pp. 180-188
[6] Zhao, C. B., *et al.*, Mineral Precipitation Associated With Vertical Fault Zones: the Interaction of Solute Advection, Diffusion and Chemical Kinetics, *Geofluids*, *7* (2007), 2, pp. 3-18
[7] Zhao, C. B., *et al.*, Theoretical and Numerical Analyses of Pore-Fluid Flow Patterns Around and Within Inclined Large Cracks and Faults, *Geophysical Journal International*, *166* (2006), 2, pp. 970-988
[8] Zhao, C. B., *et al.*, Inversely-Mapped Analytical Solutions for Flow Patterns Around and within Inclined Elliptic Inclusions in Fluid-Saturated Rocks, *Mathematical Geosciences*, *40* (2008), 2, pp. 179-197
[9] Zhao, C. B., *et al.*, Theoretical and Numerical Investigation into Roles of Geofluid Flow in Ore Forming Systems: Integrated Mass Conservation and Generic Model Approach, *Journal of Geochemical Exploration*, *106* (2010), 1, pp. 251-260
[10] Zhao, C. B., *et al.*, Mineral Precipitation Associated with Vertical Fault Zones: the Interaction of Solute Advection, Diffusion and Chemical Kinetics, *Geofluids*, *7* (2007), 3, pp. 3-18
[11] Zhao, C. B., *et al.*, Theoretical Analyses of Chemical Dissolution-Front Instability in Fluid-Saturated Porous Media under Non-Isothermal Conditions, *International Journal for Numerical and Analytical Methods in Geomechanics*, *39* (2015), 8, pp. 799-820
[12] Zhao, C. B., *et al.*, Computational Simulation of Chemical Dissolution-Front Instability in Fluid-Saturated Porous Media under Non-Isothermal Conditions, *International Journal for Numerical and Analytical Methods in Engineering*, *102* (2015), 2, pp. 135-156
[13] Zhao, C. B., *et al.*, Theoretical Analyses of Nonaqueous-Phase-Liquid Dissolution Induced Instability in Two- Dimensional Fluid-Saturated Porous Media, *International Journal for Numerical and Analytical Methods in Geomechanics*, *34* (2010), 17, pp. 1767-1796
[14] Zhao, C. B., *et al.*, Numerical Modeling of Toxic Nonaqueous-Phase-Liquid Removal from Contaminated Groundwater Systems: Mesh Effect and Discretization Error Estimation, *International Journal for Numerical and Analytical Methods in Geomechanics*, *39* (2015), 6, pp.571-593.
[15] Zhao, C. B., *et al.*, Theoretical and Numerical Analyses of Chemical-Dissolution Front Instability in Fluid-Saturated Porous Rocks, *International Journal for Numerical and Analytical Methods in Geomechanics*, *32* (2008), 9, pp. 1107-1130
[16] Zhao, C. B., *et al.*, Theoretical Analyses of Acidization-Dissolution Front Instability in Fluid-Saturated Carbonate Rocks, *International Journal for Numerical and Analytical Methods in Geomechanics*, *37* (2013), 13, pp. 2084-2105
[17] Zhao, C. B., *et al.*, A Porosity-Gradient Replacement Approach for Computational Simulation of Chemical-Dissolution Front Propagation in Fluid-Saturated Porous Media Including Pore-Fluid Compressibility, *Computational Geosciences*, *16* (2012), 3, pp. 735-755
[18] Zhao, C. B., *et al.*, Some Fundamental Issues in Computational Hydrodynamics of Mineralization, *Journal of Geochemical Exploration*, *112* (2012), 1, pp. 21-34
[19] Zhao, C. B., *et al.*, Morphological Evolution of Three-Dimensional Chemical Dissolution Front in Fluid-Saturated Porous Media: A Numerical Simulation Approach, *Geofluids*, *8* (2008), 2, pp. 113-127
[20] Zhao, C. B., *et al.*, Effects of Medium and Pore-Fluid Compressibility on Chemical-Dissolution Front Instability in Fluid-Saturated Porous Media, *International Journal for Numerical and Analytical Methods in Geomechanics*, *36* (2012), 8, pp. 1077-1100
[21] Zhao, C. B., *et al.*, Theoretical Analyses of the Effects of Solute Dispersion on Chemical-Dissolution Front Instability in Fluid-Saturated Porous Rocks, *Transport in Porous Media*, *84* (2010), 3, pp. 629-653

[22] Zhao, C. B., *et al.*, Computational Simulation for the Morphological Evolution of Nonaqueous-Phase-Liquid Dissolution Fronts in 2-D Fluid-Saturated Porous Media, *Computational Geosciences*, *15* (2011), 1, pp. 167-183
[23] Zhao, C. B., *et al.*, *Physical and Chemical Dissolution Front Instability in Porous Media: Theoretical Analyses and Computational Simulations*, Springer-Verlag, Berlin, 2014
[24] Yang, P., *et al.*, Numerical Simulation of Frost Heave With Coupled Water Freezing, Temperature and Stress Fields in Tunnel Excavation, *Computers and Geotechnics*, *33* (2006), 6-7, pp. 330-340
[25] Zhao, C. B., *et al.*, Theoretical and Numerical Analyses of Pore-Fluid Flow Focused Heat Transfer around Geological Faults and Large Cracks, *Computers and Geotechnics*, 35 (2008), 3, pp. 357-371
[26] Ma, W., *et al.*, Analyses of Temperature Fields under the Embankment with Crushed-Rock Structures along the Qinghai - Tibet Railway, *Cold Regions Science and Technology*, *53* (2012), 3, pp. 259-270
[27] Fabrice, D., *et al.*, Numerical Analysis of Seasonal Heat Storage in an Energy Pile Foundation, *Computers and Geotechnics*, *55* (2014), Jan., pp. 67-77
[28] Vanmarcke, E., Probabilistic Modeling of Soil Profiles, *Journal of the Geotechnical Engineering Division*, *103* (1977), 11, pp. 1227-1246
[29] Soulie, M., *et al.*, Modelling Spatial Variability of Soil Parameters, *Canadian Geotechnical Journal*, *27* (1990), 5, pp. 617 -630
[30] Rackwitz, R., Reviewing Probabilistic Soils Modeling, *Computers and Geotechnics*, *26* (2000), 3-4, pp. 199-223
[31] Ramly, H. E., *et al.*, Probabilistic Slope Stability Analysis for Practice, *Canadian Geotechnical Journal*, *39* (2002), 3, pp. 665-683
[32] Oktay, S., Kammer H. C., A Conduction-Cooled Module for High-Performance LSI Devices. *IBM Journal of Research and Development*, *26* (1982), 1, pp. 55-66
[33] Sluzalec, A., Temperature Field in Random Conditions, *International Journal of Heat and Mass Transfer*, *34* (1991), 1, pp. 55-58
[34] Madera, A. G., Sotnikov A. N., Method for Analyzing Stochastic Heat Transfer in a Fluid Flow, *Applied Mathematical Modelling*, *20* (1996), 8, pp. 588-592
[35] Hien, T. D., Kleiberb, M., Stochastic Finite Element Modelling in Linear Transient Heat Transfer, *Computer Methods in Applied Mechanics and Engineering*, *144* (1997), 1-2, pp. 111-124
[36] Xiu, D. B., Karniadakis, G. E., A New Stochastic Approach to Transient Heat Conduction Modeling with Uncertainty, *International Journal of Heat and Mass Transfer*, *46* (2003), 23, pp. 4681-4693
[37] Emery, A. F., Solving Stochastic Heat Transfer Problems, *Engineering Analysis with Boundary Elements*, *28* (2004), 3, pp. 279-291
[38] Vanmarcke, E., Grigoriu, M., Stochastic Finite Element Analysis of Simple Beams, *Journal of engineering mechanics*, *109* (1983), 5, pp. 1203-1214
[39] Vanmarcke, E., *Random Fields: Analysis and Synthesis*, MIT Press, Cambridge, Mass., USA, 1983
[40] Vanmarcke, E., *et al.*, Random Fields and Stochastic Finite Elements, *Structural Safety*, *3* (1986), 3-4, pp. 143-166
[41] Chen, Q., Dai, Z. M., The Isoparametric Local Average Random Field and Neumann Stochastic Finite Element Method. *Chinese Journal of Computational Mechanics*, *8* (1991), 4, pp. 397-402
[42] Liu, Z. Q., *et al.*, Random Temperature Fields of Embankment in Cold Regions, *Cold Regions Science and Technology*, *45* (2006), 2, pp. 76-82
[43] Liu, Z. Q., *et al.*, Numerical Analysis for Random Temperature Fields of Embankment in Cold Regions. *Science in China Series D: Earth Sciences*, *50* (2007), 3, pp. 404-410
[44] Wang, T., Zhou, G. Q., Neumann Stochastic Finite Element Method for Calculating Temperature Field of Frozen Soil Based on Random Field Theory. *Sciences in Cold and Arid Regions*, *5* (2013), 4, pp. 0488-0497
[45] Lewis, R. W., *et al., The Finite Element Method in Heat Transfer Analysis*, Wiley, New York, USA, 1996
[46] Zhang, J. Z., *et al.*, Methods for Characterizing Variability of Soil Parameters, *Chinese Journal of Geotechnical Engineering*, *31* (2009), 12, pp. 1936-1940
[47] Yamazaki, F., *et al.*, Neumann Expansion for Stochastic Finite Element Analysis, *Journal of Engineering Mechanics*, *114* (1988), 8, pp. 1335-1354
[48] Zhao, C. B., Valliappan, S., A Dynamic Infinite Element for Three-Dimensional Infinite-Domain Wave Problems, *International Journal for Numerical Methods in Engineering*, *36* (1993), 15, pp. 2567-2580

[49] Zhao, C. B., *Dynamic and Transient Infinite Elements: Theory and Geophysical, Geotechnical and Geoenvironmental Applications*, Springer-Verlag, Berlin, 2009
[50] Zhao, C. B., Coupled Method of Finite and Dynamic Infinite Elements for Simulating Wave Propagation in Elastic Solids Involving Infinite Domains, *Science in China Series E: Technological Sciences*, *53* (2010), 6, pp. 1678-1687
[51] Zhao, C. B., *et al.*, A Numerical Model for Wave Scattering Problems in Infinite Media Due to P And SV Wave Incidences, *International Journal for Numerical Methods in Engineering*, *33* (1992), 8, pp. 1661-1682
[52] Zhao, C. B., Computational Simulation of Wave Propagation Problems in Infinite Domains. *Science in China Series G: Physics, Mechanics and Astronomy*, *53* (2010), 8, pp. 1397-1407
[53] Zhao, C. B., Valliappan, S., Incident P and SV Wave Scattering Effects under Different Canyon Topographic and Geological Conditions, *International Journal for Numerical and Analytical Methods in Geomechanics*, *17* (1993), 2, pp. 73-94
[54] Zhao, C. B., Valliappan, S., Seismic Wave Scattering Effects under Different Canyon Topographic and Geological Conditions, *Soil Dynamics and Earthquake Engineering*, *12* (1993), 3, pp. 129-143
[55] Liu, P. L., Liu, K. G., Selection of Random Field Mesh in Finite Element Reliability Analysis, *Journal of Engineering Mechanics*, *119* (1993), 4, pp. 667-680

Paper submitted: January 13, 2017
Paper revised: August 16, 2017
Paper accepted: August 18, 2017